Seismological and SAR signature of unrest at Nisyros caldera, Greece

M. Sachpazi [a], Ch. Kontoes [a], N. Voulgaris [b], M. Laigle [c], G. Vougioukalakis [d], Olga Sikioti [a], G. Stavrakakis [a], J. Baskoutas [a], J. Kalogeras [a], J.Cl. Lepine [c]

[a] *National Observatory of Athens, Lofos Nymfon, Athens, Greece*
[b] *Department of Geology and Geothermy, Panepistimioupoli, Athens, Greece*
[c] *Laboratoire de Sismologie, Experimentale, Institut de Physique du Globe, 4 place Jussieu, 75252 Paris Cedex 05, France*
[d] *Institute of Geological and Mineral Exploration, Mesogion 70, Athens, Greece*

Abstract

Nisyros island, a Quaternary volcanic center located at the SE of the Aegean Volcanic Arc, has been in the past characterized by periods of intense seismic activity accompanied sometimes by hydrothermal explosions, the last one being in 1887. The recent long lasting episode of unrest (1995–1998) in the area is the first instrumentally documented providing information on the behavior of the volcano. Evidence from seismicity and SAR interferometry suggests that the presently active part of the Kos–Nisyros volcano-tectonic complex is located at the NW coast of Nisyros island defining an area much smaller than the whole volcano-tectonic area. Seismicity patterns vary both temporally and spatially consistently with different rates of vertical ground deformation inferred from SAR interferometry. These observations help us to discuss the different elements controlling the behavior of the volcanic system such as: the existence, location and timing of magma chamber inflation, the occurrence of tensile failure at the boundaries of the chamber and the possibility of magmatic fluids being expelled to form a shallow magmatic intrusion, the seismic failure and migration of hypocenters indicating shallow magma transport. © 2002 Elsevier Science B.V. All rights reserved.

Keywords: NE Hellenic Volcanic Arc; caldera unrest; local seismicity; SAR interferometry; magmatic inflation

1. Introduction

Signs of renewed activity at volcanic calderas are viewed with considerable interest in terms of any early and reliable recognition of precursors to an eruption. The significant increase in seismicity and ground deformation at Nisyros–Kos caldera in the period 1995–1998 was faced with considerable concern because of the generally low level of knowledge about precursors to potentially locally hazardous volcanic eruptions.

Nisyros island is part of the Aegean active Volcanic Arc, and is located at its eastern end (Fig. 1). The island represents the emerged portion of an andesitic volcano built in the last 150 000 yr, truncated by a summit caldera of 3.8 km diameter (Di Paola, 1974; Keller et al., 1990; Vougioukalakis, 1993; Francalanci et al., 1995). The caldera forming explosive activity is most probably younger than 24 000 yr BP (Keller et al., 1989). Post-caldera activity occurred as the intrusion of dacitic lava domes, raising the caldera rim to a maximum
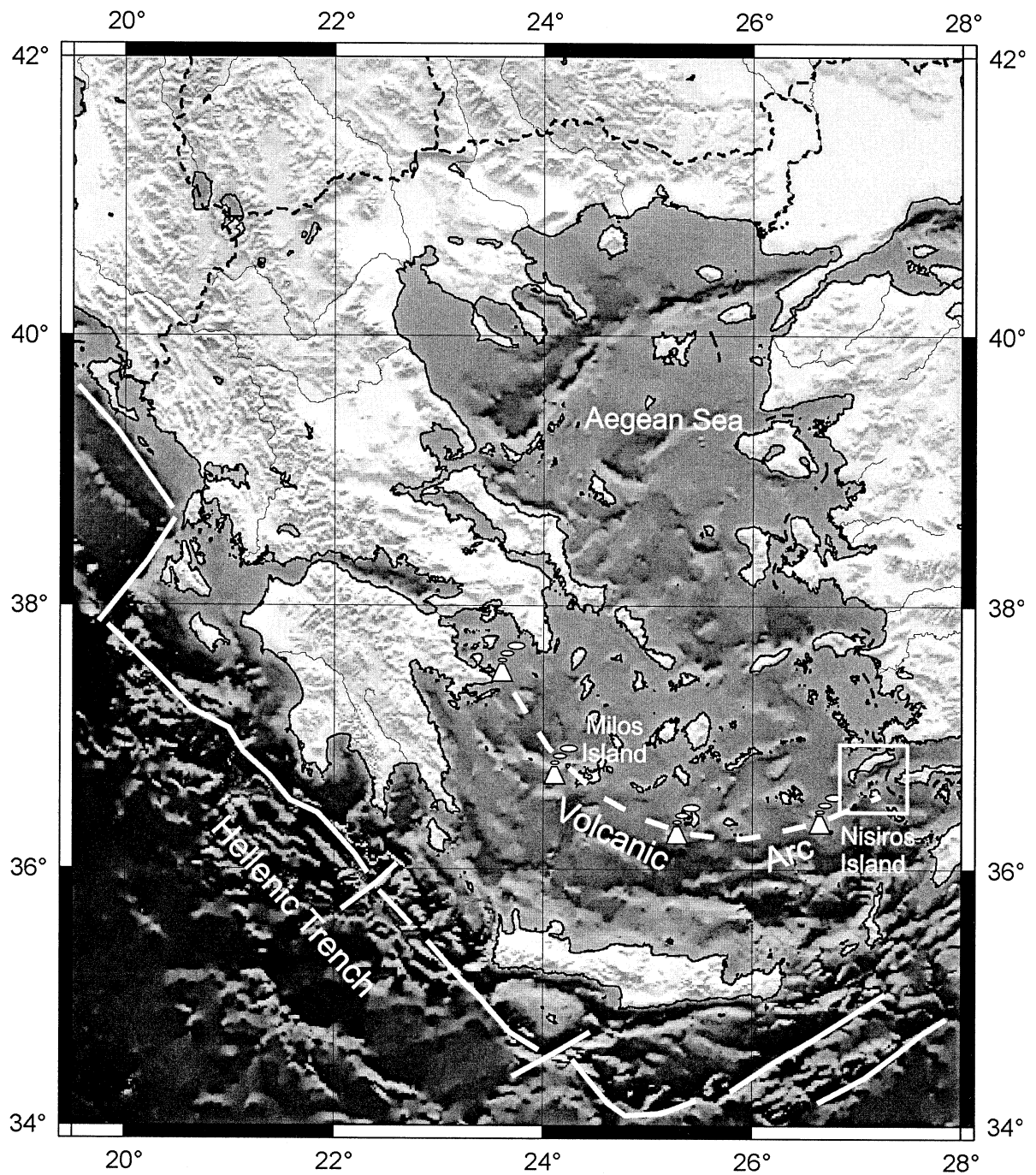
Fig. 1. Map showing (solid lines) the main units of the Hellenic trench system, the present day Volcanic Arc (triangles with dashed lines) and the position of the Nisyros volcano (square).

height of 698 m along a NE-trending tectonic. Hydrothermal explosive activity, focused in the east half of the caldera floor, produced numerous hydrothermal craters, 10 of them are well preserved (Fig. 2). Two hydrothermal eruptions have been reported during the previous century, in 1871–1873 and 1887, within the Nisyros caldera depression (Gorceix, 1873, 1874). The island is today a site of intensive hydrothermal activity which feeds many fumaroles in the caldera floor area and hot springs along the coast line. The risk of a hydrothermal explosion is high (Marini et al., 1993; Fytikas and Vougioukalakis, 1995).

Nisyros is found in the southern part of a larger and geologically more complex area, the Kos–Nisyros volcano-tectonic complex. This area is de-limited by the south Kos, the volcanic islands of Pyrgusa, Pahia, Nisyros and Strogyli, with the youngest volcanic center of the area, Yali, being at the center of this area (Keller et al., 1990; Stiros and Vougioukalakis, 1996). The whole submarine area and part of the area that today occupies north Nisyros are considered to be a large caldera collapse, triggered by the eruption of Kos plateau tuff (Dalabakis, 1987; Allen et al., 1999; Allen and Cas, 2001) (fig. 1 in Allen and Cas, 2001) before 160 000 yr (Smith et al., 1996).

At the end of 1995, intense seismic activity began on the island and lasted for about 3 years.

Seismometers were deployed temporarily in order to investigate the factors controlling the seismic behavior of the Nisyros volcano.
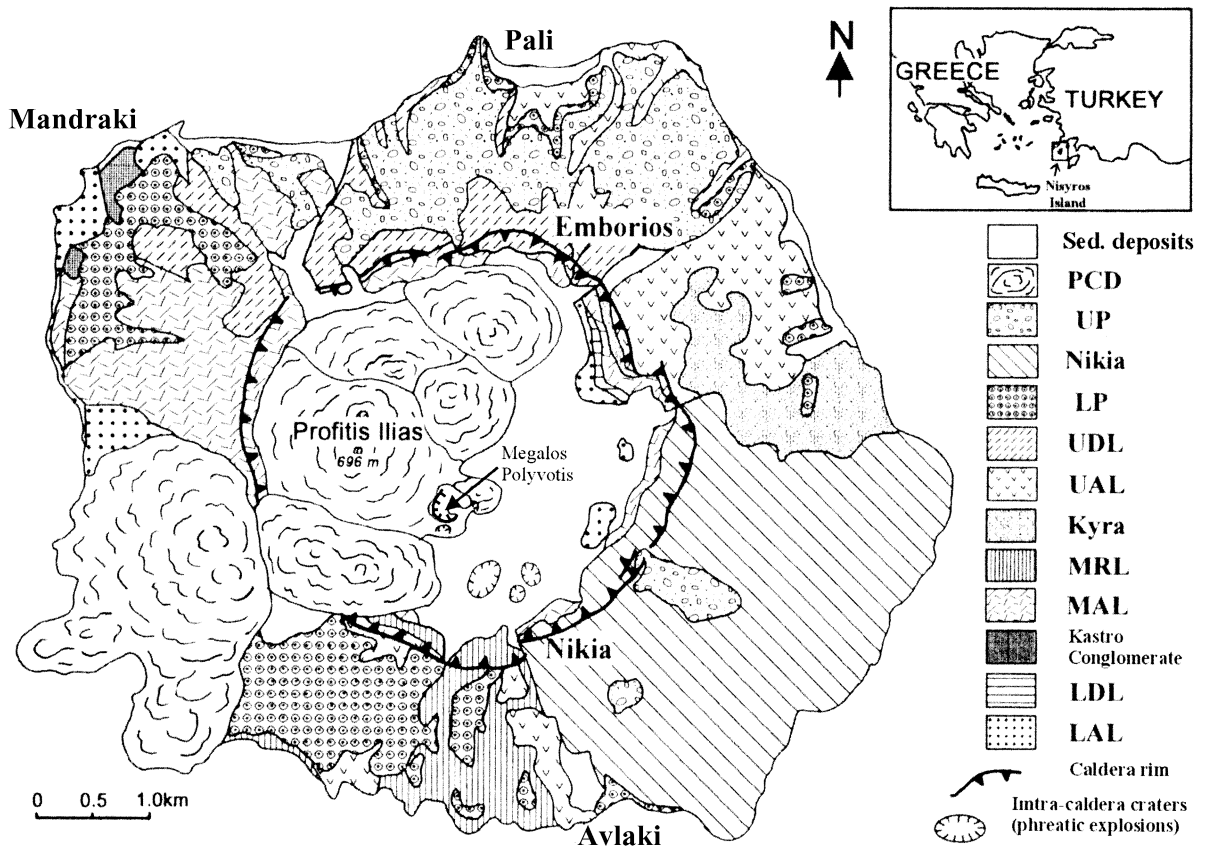
Fig. 2. Simplified geological map of Nisyros island (Vougioukalakis, 1993). The arrow indicates the area of the intense fumarolic activity of 1997.

2. Local seismicity

2.1. Historical seismicity

Nisyros has not been an important habitation center either in antiquity or more recently. For this reason there are not many detailed reports on the local seismicity, although we know that violent seismic shocks accompanied the eruptions of 1871–1873. Local swarms were also felt in Nisyros from time to time such as those of April 1887 which preceded by 5 months the last hydrothermal eruption of 1887 (Galanopoulos, 1953). Other swarms felt in Nisyros at the beginning of the century, in 1953 (Bornovas, 1953) and in 1970 (Stiros and Vougioukalakis, 1996) were not associated with any eruption (Bornovas, 1953).

2.2. Present seismicity

The background level of recorded seismicity does not seem important in this part of the arc when considering the epicenter distribution recorded by the permanent regional array for the years 1980–1994 (Fig. 3a). However, for the subsequent 4 years the number of local earthquakes is considerably higher (Fig. 3b). The earthquake activity increased during 1996, peaking in August 1997 and increasing up to the end of 1998. This is clearly seen from the diagram of Fig. 4 showing the cumulative number of the earthquakes with time. The earthquake activity declined to regular background level at the beginning of 1999 (Fig. 3c).

A local network of eight seismological stations was deployed in 1997 during two field experiments separated by 4 months. During the first experiment (25/3–3/4/97) six self-triggered three-component tape-recording seismographs were installed on Nisyros and two on Kos. During the second experiment (6/7–13/7/97) one seismograph was installed in Yali island and the others occupied mainly the same sites of the first experiment.
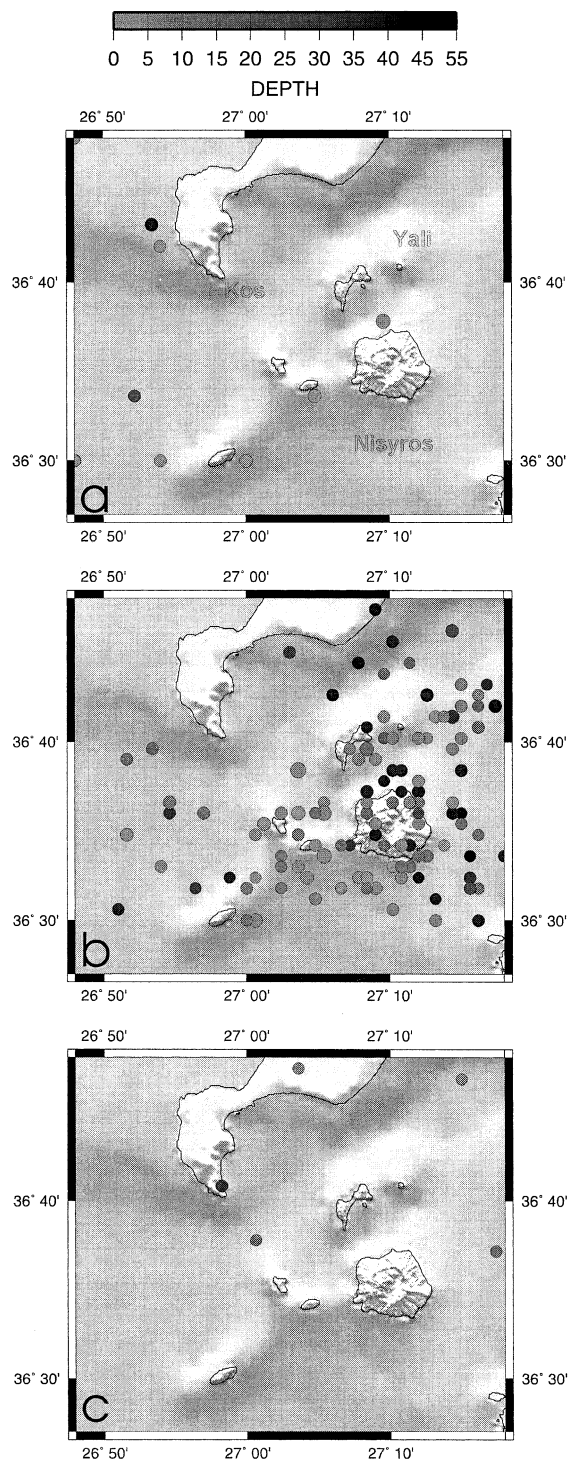
Fig. 3. Local seismicity map recorded by the National Observatory Array for the years (a) 1980–1994 (magnitudes up to 5.0), (b) 1995–1998 (magnitudes up to 5.3), (c) 1999 (magnitudes up to 4.3).
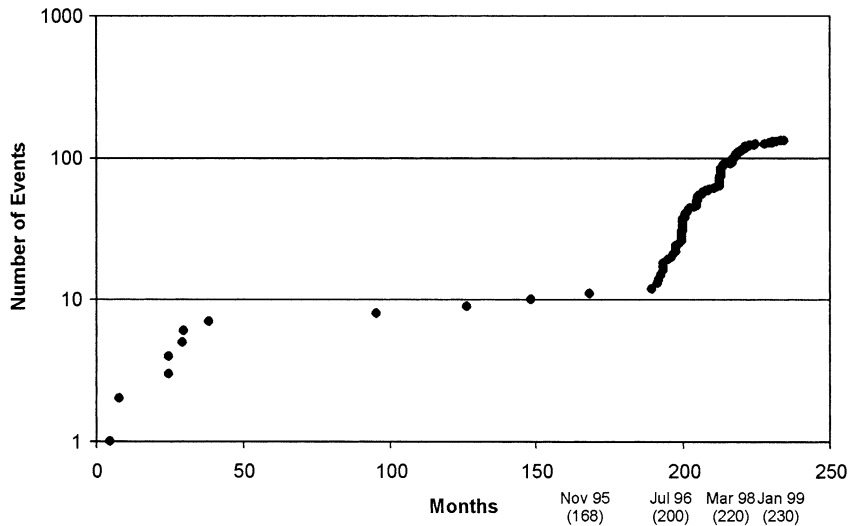
Fig. 4. Diagram showing cumulative number of earthquakes with time (1980–1999) detected by the permanent regional array.

The spatial distribution of seismic events recorded during the first period (25/3–3/4/97) is shown in Fig. 5a. Epicentral distribution shows that most earthquakes of the seismic crisis are confined in the area between the Northern coast of Nisyros and the island of Yali. The distribution of the seismicity changes for the second period of recording (6/7–13/7/97). In contrast to the spatially clustered activity of March confined to the North of Nisyros, both the central and southern parts of the island are active in July 97 providing a more dispersed seismic distribution (Fig. 5b).

The depths of the events are projected in Fig. 5c,d. The main observation is the superficial character of a large number of events from both periods with the deeper events reaching depths less than about 10 km.

2.3. Accuracy of foci locations

Test locations were run during the first stages of processing for different velocity models and for a limited number of earthquakes considering a uniform half-space medium. Independently of the model chosen, the spatial characteristics of the epicenter pattern persisted in plane.

The computed depths of the earthquakes also depend strongly on the velocity model used. To estimate the effect of variations in the velocity model on our results we re-calculated the hypocenters using different velocity models. For P-wave velocities ranging from 3 to 6 km/s, the foci of deeper events were almost independent of the velocity model with a remaining cut-off of the seismicity of about 10 km. The very superficial character of a large part of the hypocenters persists for whichever model used. However, they show a dependence on the model, exhibiting the smaller vertical location errors for the initial 5-km/s P-wave velocity model and also the smaller RMS values (Fig. 6).

Independent information on the velocity structure is provided by a marine refraction and wide angle profiling across the volcanoes of Nisyros, Yali and Kos. Makris et al. (2000) based on preliminary results propose a model for the velocity structure below Nisyros from which an average velocity of 5 km/s for the first 7–10 km can be extracted.

In Fig. 7 the best located events with errors ±1.5 km are presented for both periods of recording. The earthquake distribution for the first period of recording (March 1997) shows a concentration of epicenters (with dark dots) between the North coast of Nisyros and Yali. An aseismic offshore area southeast of Yali is apparent. It is
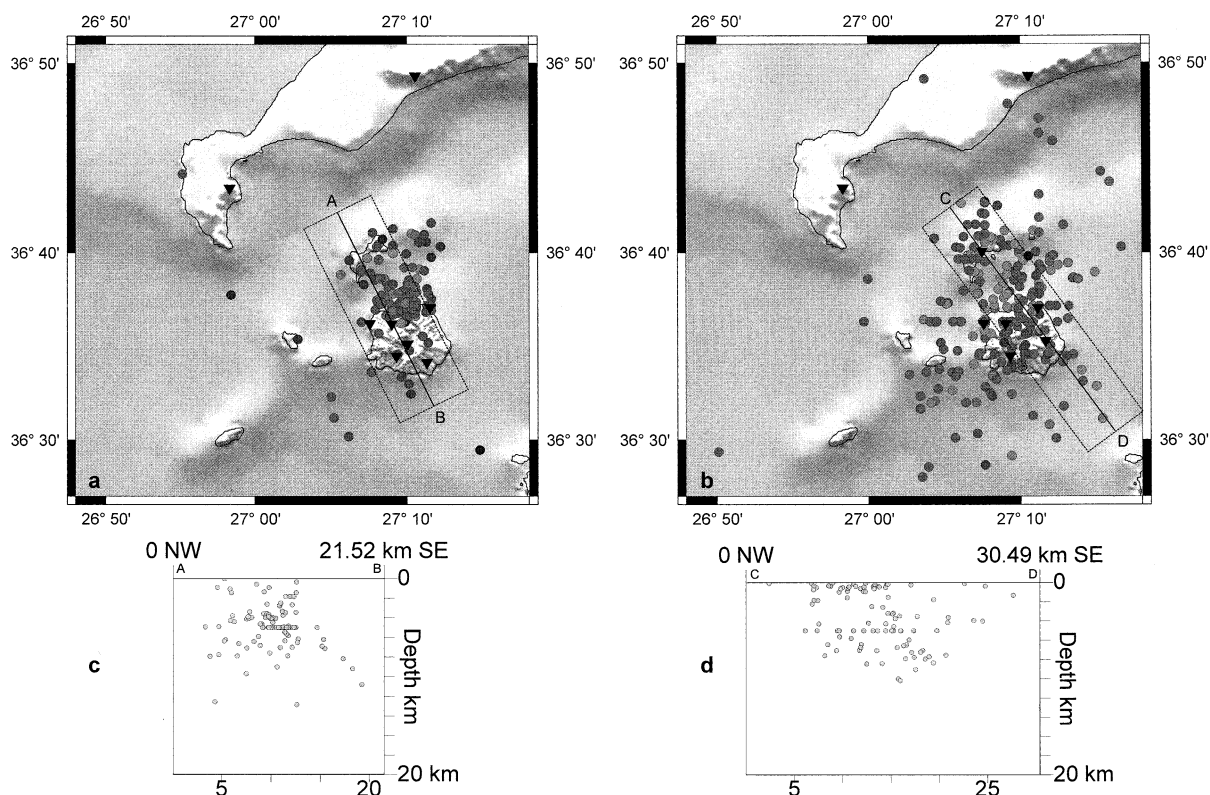
Fig. 5. Hypocentral locations resulting from a half-space velocity model of the seismic activity of March 1997. (a) Map view and (c) cross section of all the events inside the rectangle across the line AB and of July 1997. (b) Map view (d) cross section across line CD. Shown with triangles the configuration of the local temporary seismic array.

surrounded by the epicenters and hence is not an artifact of detection capacity. On the other hand, very few earthquakes are observed in the central part of the island where the onshore Nisyros caldera is situated (Fig. 2). The pattern of seismicity changed 4 months later and is shown by white dots. The data clearly indicate that new active zones appear along the central and southern part of Nisyros and also west offshore. However, the lack of epicenters persists offshore south of Yali even though bordering seismicity is now spreading out. In contrast to the seismicity of March some of the micro-earthquakes appear concentrated within the onshore caldera of Nisyros. The geometry of the array was kept mainly the same for the two periods of recording and consequently it should not prejudice the spatial trend of the earthquakes which will be discussed in relation to structure.
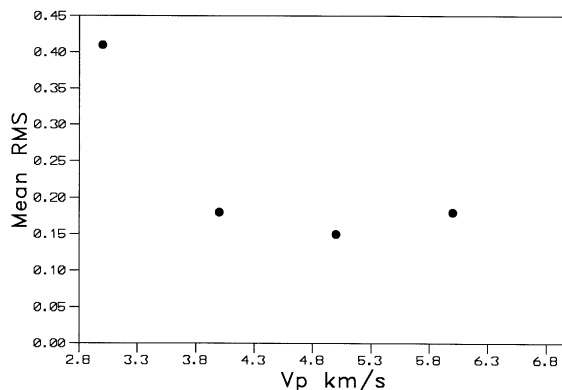
Fig. 6. Diagram showing the variation of the RMS value with different initial P-wave velocities of 3, 4, 5 and 6 km/s.
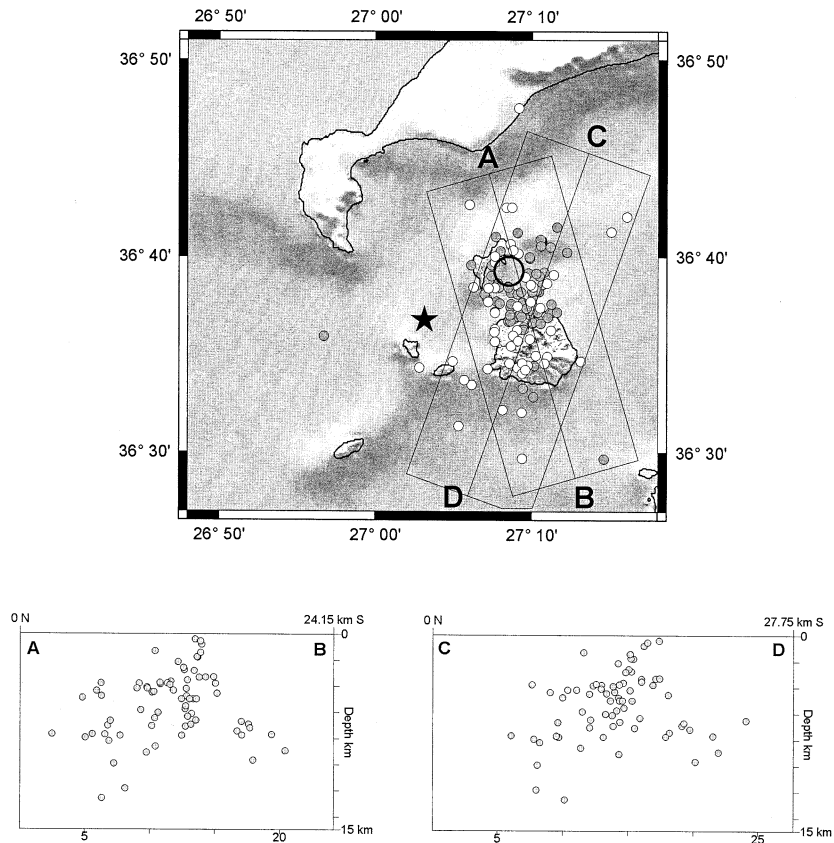
Fig. 7. (Top) Map of the best located earthquakes for the two periods shown with dark dots (March 1997) and white dots (July 1997). The star shows the location by the National Observatory regional network of the Ml = 5.3 event which occurred 28 August, 1997. (Bottom) Projections at depth of the best located events for both periods across the rectangles AB and CD. The aseismic area which persists for both periods of recording is indicated by a circle.

2.4. The distribution with magnitude

Estimation of local magnitudes was made from an analog continuous recording station. The local magnitudes were determined from the formula:

$$M = -1.01 + 1.89 \log D,$$

D is the signal duration in seconds

used by Sachpazi (1991) for the magnitude determination of Milos, another volcanic island of the South Aegean arc. The distribution of magnitudes of the events is in the range between 0.7 and 2.1 R.

It is usual in seismological research to consider the repartition of energy release among the shocks in a swarm. The standard relation:

$$\log N = a - bM$$

(with M the magnitude and N the number of events with magnitude equal or larger than M) is used. Currently the parameter b is considered to characterize the degree of heterogeneity of structure or stress as shown in laboratory measurement of acoustic emission of failure of stressed rocks (e.g. Mogi, 1967) or the fractal dimension of the faulting elements. Essentially, the so-called tectonic earthquakes have a characteristic small b value, close to 1, often even closer to

0.5 while earthquakes occurring in volcanic and geothermal areas exhibit higher *b* values reaching up to *b* = 2 (Warren and Latham, 1970). Papadopoulos et al., 1998 found a *b* value of 1.67 for Nisyros area considering however a very small data set of about 60 micro-earthquakes.

The *b* coefficient was computed from a set of 107 micro-earthquakes recorded during March 1997 and for another set of 350 micro-earthquakes recorded 4 months later (Fig. 8). For both periods we obtain similar values of *b* = 1. At a first order this shows that there is no *b* value variation as a function of time. However, the location of seismicity in the two different experiments shifts so that we do not cover the same volume at different times. Wyss et al., 1997 find a *b* value of 1.5 and correlate it to the presence of an active magma chamber beneath the off-Ito volcano in Japan. The authors document an increase

of the *b* value from 0.7 to 1.5 in a period of 10 yr and interpret it as a trend of increasing crack density due to intrusion activity. It is clear that in our case we do not have appropriate data accuracy in order to recover reliable information contained in the *b* value and discuss its relation with the numerous factors which can modify it.

3. Ground deformations by SAR interferometry

Interferometric analysis of SAR images has demonstrated potential to monitor, measure and map crust deformations associated to earthquakes, volcanic activity and other geophysical phenomena (Zebker et al., 1994; Peltzer and Rosen, 1995; Massonnet and Feigl, 1995; Murakami et al., 1996; Thatcher and Massonnet, 1997; Massonnet and Feigl, 1998). The technique was used by Massonnet et al. (1995) to measure the deflation induced by the activation of Etna volcano in the time period from May 17, 1992 to October 24, 1993. Additionally, the deformation field associated to the 1997 eruption of Okmok volcano in Alaska (Lu et al., 1998), as well as the Campi Flegrei caldera activation (Avallone et al., 1999) were measured by constructing interferograms from the phase difference of ERS SAR images.

The interferometric calculations were based on the use of ERS-2 SAR images spanning the period from June 4, 1995 to June 8, 1997. From these interferograms it is demonstrated that a continuous vertical deformation of the surface of Nisyros island occurred in the period between acquisition of the two images. The satellite images were acquired at the ascending pass of the ERS-2 system, where the satellite travels approximately from south to north looking eastwards and inclined 23.5° from the vertical. The selection of the interferometric pairs to process was based on their sensitivity to the topography, expressed by the altitude of ambiguity. As the radar observes a target by two slightly different points of view there is a stereoscopic effect yielding fringes called 'topographic fringes', having the form of contour lines. The altitude of ambiguity (h_a) is the parameter that gives an order of magnitude in the
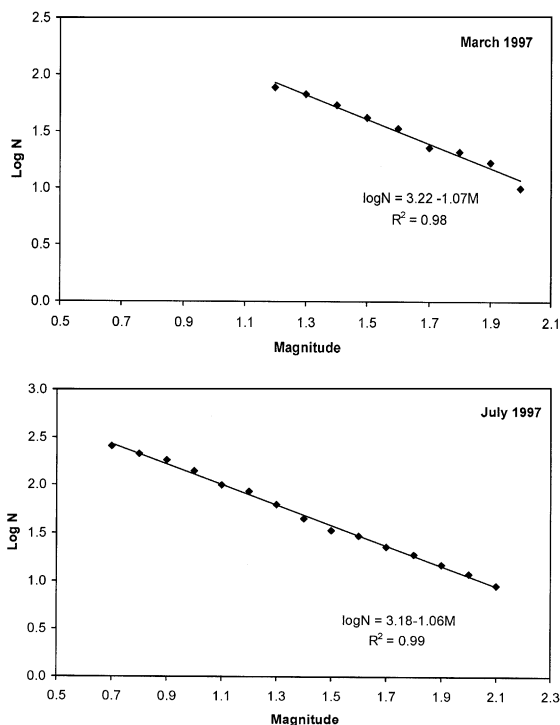
Fig. 8. Gutenberg–Richter diagrams of Nisyros local seismicity for (in the top) a set of 107 micro-earthquakes recorded in March 1997 and (in the bottom) a set of 350 micro-earthquakes recorded in July 1997. No variation of *b* value (close to 1) is observed between the two periods.

change of altitude needed to produce one topographic fringe (Massonnet and Feigl, 1998). This parameter becomes very essential when the topographic fringes produced from an existing Digital Elevation Model (DEM) are to be used to eliminate the topography from the calculated interferograms, keeping only fringes relative to the surface deformations. In this case, if the DEM's inherent errors are close to the magnitude of h_a, it becomes evident that there will be remaining residual topographic fringes in the interferograms. Consequently, the greater the value of h_a, compared to the DEM's inherent errors, the lower the likelihood to get an interferogram affected by residual topographic fringes. In practice, h_a values between 50 and 250 m result in small stereoscopic effects considering that a rather accurate DEM (± 10–20 m) is used. Such a combination yields moderate topographic fringes and much more reliable estimations of the ground deformation field. Table 1 illustrates the time spanning of the interferometric pairs used, as well as their corresponding h_a values and baseline perpendicular lengths.

In this study, a DEM was produced by digitizing contour lines and spot height data from existing 1:5000-scale topographic maps achieving a height accuracy of the order of ± 10 m, tested by a set of independent control points of known elevation. Therefore, the magnitude of the expected topographic artifacts expressed in phase cycles, for the worst interferometric pair ($h_a = 64$ m), was of the order RMS/$h_a = 10$ m/64 m = 0.16 phase cycles or 4.375 mm in range. The same calculation for the best pair ($h_a = 180$ m) yielded 0.055 cycles, that is equivalent to 1.55 mm in range. This simply means that in each fringe representing a change in the slant range direction of 28 mm the maximum inherent estimation error is of the order of 4.375 mm or equivalent 15%, in

the case of the worst interferometric pair. The same error in estimations and for the best interferometric pair is of the order of 1.55 mm or 5%.

The differential interferometry survey makes evident that significant crust deformations occurred on the surface of Nisyros island during the years 1995–1997. The calculated interferograms demonstrate a continuous surface movement in the same direction. The observed deformation field shows an approximately circular shape centered at the NW of Nisyros. In the interferogram of Fig. 9a spanning the period June 4, 1995 to May 19, 1996, three fringes are shown, though partly interrupted by the surrounded sea, indicating a change in the slant range direction of the order of 84 mm. In the year that follows (1996–1997) the surface keeps moving with the same trend. The two resulted fringes of the corresponding interferogram spanning the period May 19, 1996 to June 8, 1997 indicate a further surface displacement of 56 mm in range (Fig. 9b). Generally for the 2-yr period spanning June 4, 1995 to June 8, 1997, the surface unceasing movement keeps a constant displacement trend along the slant range direction and a circular fringe pattern (Fig. 9c). It is also worth noting that the comparison of this interferogram with the ones spanning the periods June 4, 1995 to May 19, 1996 and May 19, 1996 to June 8, 1997 yields that the number of the fringes equals the sum of the fringes in the two shorter periods.

As already mentioned, SAR interferometry gives slant range deformations including both a vertical and a horizontal component. However, the vertical component predominates due to the specific small angle of incidence for the ERS sensor (average 23° from the vertical). Consequently, the vertical movement generally predominates in the interferograms. It should be noted, however,

Table 1
ERS-2 image pairs used for interferometric calculations

Acq. date image 1	Acq. date image 2	Altitude of ambiguity h_a (m)	Satellite orbits	Baseline perpendicular length	Estimated mean coherence value	Figure code
4/06/1995	19/05/1996	99	641–5651	102	0.46	Plate 1a
19/05/1996	8/06/1997	180	5651–11162	56	0.65	Plate 1b
4/06/1995	8/06/1997	64	641–11162	158	0.64	Plate 1c
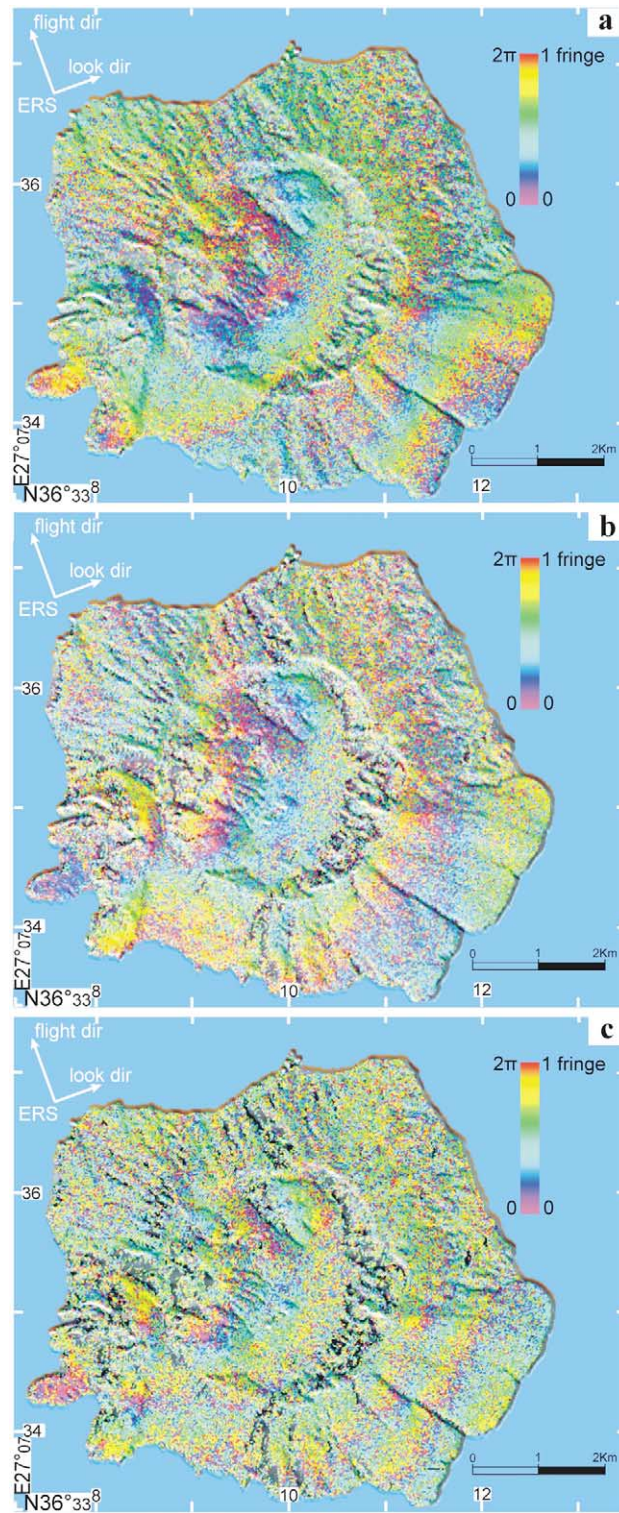
that in order to separate horizontal and vertical displacements, the slant range-projected deformations by themselves are not enough. Additional information from external sources (e.g. GPS survey) is required.

In order to cross-check the displacement observations described before, additional radar images, acquired in the descending pass of the ERS-2 satellite, were used in dates close to the ones of the ascending pass. The interferograms produced showed similar fringe patterns as the ascending pass images. Nevertheless, the resulted fringes were less clear especially due to lower coherence, higher layover and shadow discontinuities present on the available image data. As a general remark, the descending pass viewing geometry seemed less favorable to map the surface of the island. However, it must be noted that the interferometric pairs produced from descending pass images confirmed both the pattern and trend of the deformation field observed in ascending pass images.

Calculating coherence values for every pixel of the interferograms provided additional estimation of the reliability level of the results. Theoretically coherence values range between 0 and 1 and map the intrinsic coherence (physical properties) of the ground during the acquisition dates of the two images used for interferometric calculations. A default threshold value in the processing has been set to 0.4. This value has proven to be optimal for not introducing noise. Therefore pixels not reaching this threshold level were not considered for further processing and were masked out. Table 1 illustrates mean coherence values estimated for each interferometric pair.

From this interferometric analysis, it becomes evident that the recent unrest at Nisyros in the period 1995–1997 resulted in easily detected crust deformations of the order of 140 mm. In this deformation, there is a very small fraction of 7 mm (5% of the total deformation) which is due to topographic artifacts, as explained before. This fraction is considered negligible compared to the total amount of deformation so as to be taken into account in the results.

The rate of change was rather higher in the period 1995–1996, reaching an average value of 87 mm/yr. During the second studied period (1996–1997), the process of surface deformation was still continuing but at a rate which tended to decrease with time (53 mm/yr). The observed changes along the viewing axis of the satellite represent an unceasing movement of the ground in the period 1995–1997 keeping a constant uplift trend with varying deformation rate. These results were in conformity with the ones of the study of Lagios et al. (1998), where GPS measurements were applied on the Nisyros island in 1997. These measurements concluded that the area was submitted to a general surface uplift trend. It should be noted, however, that in general GPS measurements give better results in the horizontal component of the deformation field, whereas interferometry is more sensitive to vertical movements due to small incidence angles, e.g. $\sim 23.5°$ for the ERS satellites. This is the reason why interferometric observations are usually complementary to GPS measurements of a local dense network performing a continuous monitoring of horizontal movements. However, in the case of Nisyros the only known GPS data available (Lagios et al., 1998) were corresponding to two interval times within 1997, which did not coincide with the acquisition dates of the SAR images used for this year. Furthermore, these data could not be extrapolated and compared to the interferometric results, which in their turn cover the full period between 1995 and 1997. Consequently, it was decided to simply combine the two sets, getting from the interferograms a more accurate image of the temporal and spatial coverage characteristics of the deformations and from the GPS data the absolute sign of the trend indicating a general surface uplift.

Fig. 9. Interferograms calculated by the phase difference of SAR images recorded by ERS satellite for the period from June 4, 1995 to June 8, 1997. A continuous surface movement with an approximately circular shape is observed with its center to the NW coast of the island. (a) Three fringes are shown for the period of June 4, 1995 to May 19, 1996, indicating a ground deformation in slant range direction of the order of 84 mm. (b) Two fringes are shown for the period of May 19, 1996 to June 8, 1997, indicating a further surface displacement of 56 mm. (c) Five fringes of 140 mm occurred in the period 1995–1997.

4. Temporal and spatial evolution of the 1995–1997 event

A temporary array of an adequate geometry should allow accurate locations to a kilometric resolution necessary to discuss activity and volcano structure. Thus, the spatial trend of the earthquakes may be considered in relation to the existence of this magma chamber. Both periods of seismic recording suggest the presence of an aseismic area south of Yali. This may be interpreted in terms of material of low strength and cohesion consistent with the location of a volume of magma. The existence of a volcanic intrusion in the same area is also supported by velocity modeling of active seismic investigations that took place in the area (Makris and Chonia, 1999). This intrusion is located about 7 km NNE of the center of the uplift area and could have been extruded from a larger magma chamber. Indeed McTigue (1987) argues for the tensile failure of a magma chamber so that magmatic fluids can be expelled, generally not from the top of the inflating chamber, but where the influence of the free surface combines with it, for maximum hoop stress. If the aseismic area south of Yali indeed corresponds to such a magmatic volume, its intrusion should have occurred before the first period of seismic recording (in March 1997). It appears likely that this could have been in the earlier stage of this unrest episode which began at the end of 1995, before local seismicity could be monitored in 1997. Indeed, it is in the earliest period, of 1995–1996, that the maximum rate of line-of-sight deformation was observed by SAR interferometry, reaching 87 mm/yr, with respect to 53 mm/yr for the period 1996–1997. It is also during this first period that earthquakes began to be felt by the local inhabitants, with magnitudes reaching 4 and 5 on the Richter scale. Vougioukalakis et al. (1998) report a 2–3-cm opening, in April 1996, of an almost N–S-trending fracture in Mandraki (Fig. 2) as the source of seismic damage effects observed in the local buildings and also of a N140–155 fracturing on Yali island which opened 3 months later (July 1996). Both faults have been reactivated in the past (1873 and 1970 respectively) during a similar crisis (Vougioukalakis et al., 1998). We propose that these earthquakes were caused by the addition to the regional stress field of new magmatic pressure. This is expected to be important right above the top of the chamber, next to Mandraki and conformingly to the regional extensional stress field (Jackson et al., 1982) the maximum compressive stress axis would be vertical and normal faulting would occur. No reliable focal mechanism is available for the events occurring at the area of maximum vertical deformation to test our hypothesis. The best constrained local mechanisms showed compression in the central part of the quadrant (Fig. 10a) which is inconsistent with normal faulting. However, the location of the five events, further away from the top of the magma chamber, suggests a more oblique direction for the maximum compressive axis and may explain the strike slip mechanism controlling the event occurrence (Fig. 10b).

The earthquake distribution of the second period of recording in July 1997 indicates the activation of new zones to the south with most of the micro-earthquakes concentrated within the on-shore caldera of Nisyros. This was also detected during the soil gas survey of the area. The Radon content registered in the fumaroles and soil gasses of the caldera floor was the maximum during the whole crisis (4500 pCi/l). After this period it continuously declined, arriving at less than 300 pCi/l in the 2000 survey. Increased fumarolic activity was also observed from June to September 1997. Intense fumarolic activity appeared specifically in the south flanks of the Megalos Polivotis hydrothermal crater. The intensification of the fumarolic activity took place on August 28, 1997, 1 day after the occurrence of the two strongest earthquakes (Ml 5.3 and 5.2) since the beginning of the unrest phase earthquakes. Seismic events located by the local array operating 1 month earlier in this area may be indicators of the transport of magmatic fluids from the NW coast where the maximum ground deformation is detected, towards the central south where we can find very shallow located aquifers heated by steam (Chiodini et al., 1993). We suggest that the activation of the hydrothermal feeding faults by the earthquakes favored the ascent of steam from aquifers to the surface, creating the intensification of the

fumarolic activity. The major earthquakes could only be located with distant stations of the National Observatory network. Computed epicenters are situated offshore, about 5–8 km west of the onshore caldera. This is well within the range of uncertainty, since the studied area is at the extremity of the Greek Regional array and consequently its capacity for resolution is limited compared to that of the local array, concerning the hypocentral coordinates.
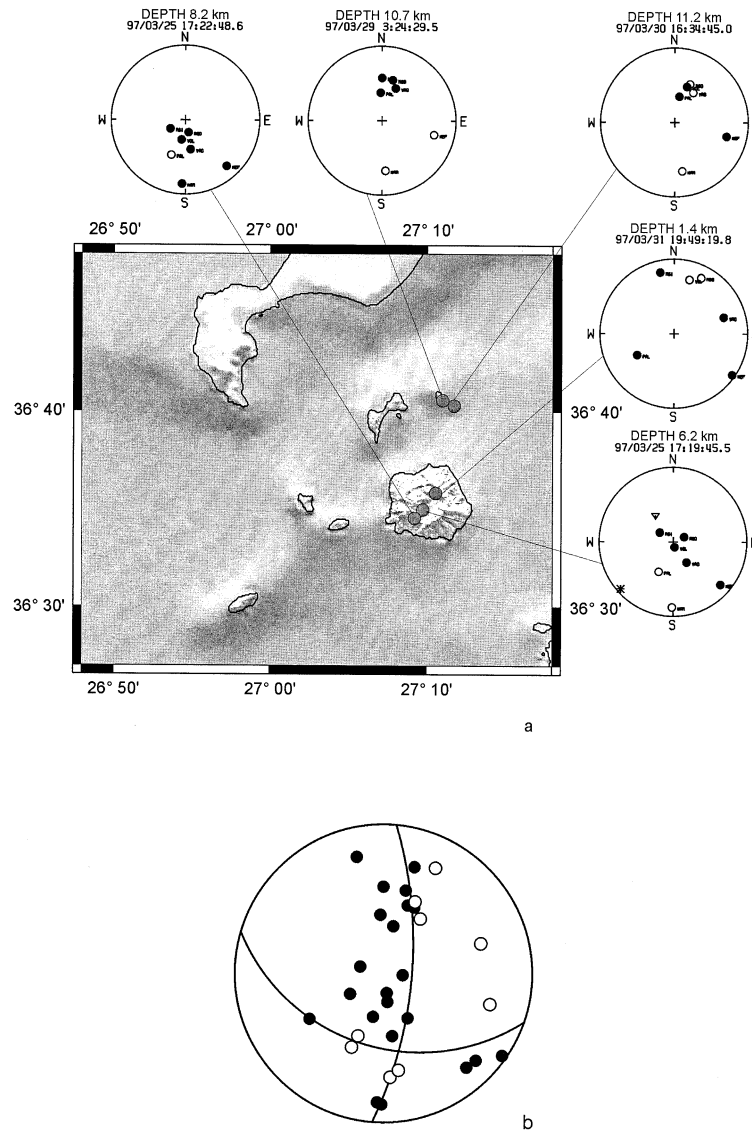
Fig. 10. (a) Plots of the first polarities distribution for five selected earthquakes. Open circles indicate dilatations and closed circles compressions. Located away of the maximum uplift area where one might expect a vertical maximum compressive stress axis consistently to the regional extensional field, the events exhibit a mechanism with a more oblique maximum compressive axis. A close-map shows the locations and depths for the five events (b) composite mechanism.

5. Summary and conclusions

The study of the spatial and temporal character of seismic activity together with the monitoring of ground deformation by SAR interferometry during the present episode of 1995–1997, highlights different phases of an intense unrest period of this area at the SE part of the Volcanic Arc. The study of the interferograms shows a continuous deformation of the order of 140 mm during 1995–1997 with its maximum occurring at the northwest part of the island. Consistently with observations in other volcanic calderas in a state of unrest e.g. Campi Flegrei, Italy (De Natale et al., 1995), Rabaul, New Guinea (McKee et al., 1984), deformation may be attributed to Mogi-type inflation of a magma chamber. Keller et al. (1990) support the existence of a large eruptive center located offshore south of Kos. According to them this area hosted at 0.14 Ma the most violent explosive event in Quaternary Aegean volcanism which produced more than 100 km^3 of magma. Dalabakis (1987) places a caldera with a diameter of at least 5–10 km near the recent volcanoes of Nisyros and Yali. SAR data suggest the existence of a magma chamber with its top at the northwest part of Nisyros. Inflation of this chamber may be responsible for the unrest episode observed in 1995–1997 resulting in important ground deformation and also intense seismic activity. The observed faulting in the island which has been the source of serious house damage is then probably induced as a secondary effect of the pressure increase above the magma chamber.

It is interesting to point out that the northwest edge of Nisyros island is a tectonic block which suffered the maximum uplift in the geological history of the island. In this part outcrop the uplifted submarine basement of the island (Di Paola, 1974) and large and rapid uplift movements in the last 3000–4000 years have also been detected (Stiros, 2000).

No eruption followed this important unrest episode, in contrast to that of 1871–1873. However, the example of Rabaul caldera in Papua-New Guinea where an eruption took place 10 years after the last period of unrest (Gudmundsson et al., 1999) confirms the complexity of the volcano controlling mechanism and consistently implies that geophysical monitoring in this part of the Hellenic Volcanic Arc is necessary not only during episodes of alarming activity but through the intervening apparently quiescent periods as well. Indeed, without observations made in periods of quiet, the beginning of unrest may pass unnoticed.

References

Allen, S.R., Cas, R.A.F., 2001. Transport of pyroclastic flows across the sea during the explosive, rhyolitic eruption of the Kos Plateau Tuff, Greece. Bull. Volcanol. 62, 441–456.

Allen, S.R., Stadlbauer, E., Keller, J., 1999. Stratigraphy of the Kos Plateau Tuff: Products of a major Quaternary explosive rhyolitic eruption in the eastern Aegean Sea. Int. J. Earth Sci. 88, 132–156.

Avallone, A., Zollo, A., Briole, P., Delacourt, C., Beauducel, F., 1999. Subsidence of Campi Flegrei (Italy) detected by SAR interferometry. Geophys. Res. Lett. 26, 2303–2306.

Bornovas, J., 1953. On the earthquakes of Nisyros in January 1953. Unpublished report, Institute of Geology and Mineral Exploration, Athens (in Greek).

Chiodini, G., Cioni, R., Leonis, C., Marini, L., Raco, B., 1993. Fluid geochemistry of Nisyros Island, Dodecanese, Greece. J. Volcanol. Geotherm. Res. 56, 95–112.

Dalabakis, P., 1987. Une des plus puissantes eruptions phréatomagmatiques dans la Mediterranée orientale: l'Ignimbrite de Kos (Greece). C.R. Acad. Sci. Paris 303 (Serie II), 505–508.

De Natale, G., Zollo, A., Virieux, J., Ferraro, A., 1995. Accurate fault mechanism determinations for a 1984 earthquake swarm at Campi Flegrei caldera (Italy) during an unrest episode: Implications for volcanological research. J. Geophys. Res. 100 (B12), 24167–24185.

Di Paola, G.M., 1974. Volcanology and petrology of Nisyros Island (Dodecanese, Greece). Bull. Volcanol. 38, 944–987.

Francalanci, L., Varecamp, J.C., Vougioukalakis, G., Defant, M.J., Innocenti, F., Manetti, P., 1995. Intricate processes occurring in the convecting, fractionating and assimilating magma chamber of Nisyros volcano, Aegean arc, Greece. Bull. Volcanol. 56, 601–620.

Fytikas, M., Vougioukalakis, G., 1995. Volcanic hazard in the Aegean Islands. In: Horlick-Jones, T., Amendola, A., Casale, R. (Eds.), Natural Risk and Civil Protection. Spon, Brussels, pp. 117–130.

Galanopoulos, A., 1953. Katalog der Erdbeben in Griechen-

land für die Zeit von 1879 bis 1892. Ann. Geol. Pays Hellen. 5, 144–229.

Gorceix, M.H., 1873. Sur la récente éruption de Nisyros. C.R. Acad. Sci. Paris 77, 1039.

Gorceix, M.H., 1874. Phénomènes volcaniques de Nisyros. C.R. Acad. Sci. Paris 78, 444–446.

Gudmundsson, O., Johnson, R.W., Finlayson, D.M., Nishi-mura, Y., Shimamura, H., Terashima, A., Itikarai, I., Thurber, C., 1999. Multinational seismic investigation focuses on Rabaul Volcano. EOS Trans. Am. Geophys. Union 80-24, 272–273.

Jackson, J.A., King, G., Vita-Finzi, C., 1982. The neotectonics of the Aegean: An alternative view. Earth Planet. Sci. Lett. 61, 303–318.

Keller, J., Gillot, P.Y., Rehren, Th., Stadlbauer, E., 1989. Chronostratigraphic data for the volcanism in the eastern Hellenic arc Nisyros and Kos. Terra Abstr. 1, 354.

Keller, J., Rehren, Th., Stadlbauer, E., 1990. Explosive volcan-ism in the Hellenic arc: A summary and review. Proceedings of the third International Congress, Thera and the Aegean World III, Vol. 2, pp. 13–26.

Lagios, E., Chailas, S., Giannopoulos, I., Sotiropoulos, P., 1998. Surveillance of the Nisyros volcano. Establishment and remeasurement of GPS and Radon networks (in Greek with English abstract). Bull. Geol. Soc. Greece 32, 215–227.

Lu, Z., Mann, D., Freymueller, J., 1998. Satellite radar inter-ferometry measures deformation at Okmok volcano. EOS Trans. Am. Geophys. Union 79, 461–468.

Makris, J., Chonia, T., 1999. Active and passive seismic studies of Nisyros volcano-east Aegean Sea. Proceedings of 1999 CCSS Workshop, Dublin, Ireland. Communication of the Dublin Institute for Advance Studies. Series D, Geophysical Bulletin No. 49, pp. 9–12.

Marini, L., Principe, C., Chiodini, G., Cioni, R., Fytikas, M., Marinelli, G., 1993. Hydrothermal eruptions of Nisyros (Dodecanese, Greece): Past events and present hazard. J. Volcanol. Geotherm. Res. 56, 71–94.

Massonnet, D., Feigl, K., 1995. Discrimination of geophysical phenomena in satellite radar interferograms. Geophys. Res. Lett. 22, 1537–1540.

Massonnet, D., Feigl, K., 1998. Radar interferometry and its applications to changes in the earth's surface. Rev. Geophys. 36, 441–500.

Massonnet, D., Briole, P., Arnaud, A., 1995. Deflation of Mount Etna monitored by spaceborne radar interferometry. Nature 375, 567–570.

McKee, C.O., Lowenstein, P.L., De Saint Ours, P., Talai, B., Itikarai, I., Mori, J.J., 1984. Seismic and ground deforma-tion crises at Rabaul Caldera: Prelude to an eruption? Bull. Volcanol. 47, 397–411.

McTigue, D.F., 1987. Elastic stress and deformation near a finite spherical magma body: Resolution of the point source paradox. J. Geophys. Res. 92, 12931–12940.

Mogi, K., 1967. Earthquakes and fractures. Tectonophysics 5, 35–55.

Murakami, M., Tobita, M., Fujiwara, S., Saito, T., Masaharu, H., 1996. Co-seismic crustal deformations of the 1994 Northridge, California, earthquake detected by interferomet-ric JERS 1 Synthetic Aperture Radar. J. Geophys. Res. 101, 8605–8614.

Papadopoulos, G., Sachpazi, M., Panopoulou, G., Stavraka-kis, G., 1998. The volcanoseismic crisis of 1996–97 in Ni-syros, SE Aegean Sea, Greece. Terra Nova 10, 151–154.

Peltzer, G., Rosen, P., 1995. Surface displacements of the 17 May 1993 Eureka Valley, California, earthquake observed by SAR interferometry. Science 268, 1333–1336.

Sachpazi, M., 1991. Etude Sismologique de la Structure et du Champ Geothermique de l'Ile de Milos (Greece) avec un Reseau Dense de Stations Sismique Latge Bande. Unpub-lished Doctoral Thesis, Université de Paris VII, Paris.

Smith, P.E., York, D., Chen, Y., Evensen, N.M., 1996. Single crystal ^{40}Ar–^{39}Ar dating of a Late Quaternay paroxysm on Kos, Greece: Concordance of terrestrial and marine ages. Geophys. Res. Lett. 23, 3047–3050.

Stiros, S.C., 2000. Fault pattern of Nisyros Island volcano (Aegean Sea, Greece): Structural, coastal and archaeological evidence. In: McGuire, W.J., Griffiths, D.R., Hancock, P.L., Stewart, I.S. (Eds.), The Archaeology of Geological Cata-strophes. Geological Society, London, Special Publications 171, 385–397.

Stiros, S.C., Vougioukalakis, G., 1996. The 1970 Yali (SE edge of the Aegean volcanic arc) earthquake swarm: Surface faulting associated with a small earthquake. Ann. Tecton. X, 20–30.

Thatcher, W., Massonnet, D., 1997. Crustal deformation at Long Valley caldera, eastern California, 1992–1996 inferred from satellite radar interferometry. Geophys. Res. Lett. 24, 2519–2522.

Vougioukalakis, G., 1993. Volcanic stratigraphy and evolution of Nisyros island (in Greek with English abstract). Bull. Geol. Soc. Greece 28, 239–258.

Vougioukalakis, G., Sachpazi, M., Perissoratis, K., Liberopou-lou, Th., 1998. The 1995–1997 seismic crisis and ground deformation on Nisyros volcano, Greece: a volcanic unrest? 6th Int. Meeting on Colima volcano, Abstracts Vol.

Warren, N.W., Latham, G.V., 1970. An experimental study of thermally induced microfracturing and its relation to vol-canic seismicity. J. Geophys. Res. 75, 4455–4464.

Wyss, M., Shimazaki, K., Wiemer, S., 1997. Mapping active magma chambers by b values beneath the off-Ito volcano, Japan. J. Geophys. Res. 102 (B9), 20413–20422.

Zebker, H.A., Rosen, P.A., Goldstein, R.M., Gabriel, A., Werner, C.L., 1994. On the derivation of co-seismic dis-placement fields using differential radar interferometry: The Landers earthquake. J. Geophys. Res. 99, 19617–19634.